

Rectangular lattices of permalloy nanoparticles: Interplay of single-particle magnetization distribution and interparticle interaction

A. A. Fraerman, S. A. Gusev, L. A. Mazo, I. M. Nefedov, Yu. N. Nozdrin,

I. R. Karetnikova, M. V. Sapozhnikov,* I. A. Shereshevskii, and L. V. Sukhodoev

Russian Academy of Science, Institute for Physics of Microstructures GSP-105, Nizhny Novgorod, 603600, Russia

(Received 11 May 2001; published 22 January 2002)

Regular two-dimensional rectangular lattices of permalloy nanoparticles (40 nm in diameter) were prepared by electron lithography. The magnetization curves were studied by differential Hall magnetometry for different external field orientations at 4.2 and 77 K. The shape of the hysteresis curves indicates that there is magnetostatic interaction between the particles. The main peculiarity of the system is the existence of remanent magnetization perpendicular to the easy plane. By numerical simulation it is shown that the feature of the magnetization reversal is a result of the interplay of the interparticle interaction and the magnetization distribution within the particles (vortex or uniform).

DOI: 10.1103/PhysRevB.65.064424

PACS number(s): 75.75.+a, 75.60.-d

I. INTRODUCTION

It is now well known that the competition between magnetostatic and exchange energy in a very small (~ 20 nm) particle leads to a single-domain state. If the radius of a particle is sufficiently large, a nonuniform distribution of magnetization has a minimal energy. It is a vortex in an isotropic magnetic disk. Such a particle was referred to as a circular nanomagnet.¹ In the case of an individual nanoparticle the vortex has a perpendicularly magnetized core.² Nowadays the vortex distribution of magnetization in nanomagnets is under detailed investigation.³ Such systems are considered as perspective for use in RAM (random access memory) devices.⁴ It is obvious that the distribution of magnetization in nanomagnets depends on the interaction between particles. The fundamental type of interaction, which can lead to long-range ordering⁵ and to collective behavior in the system of particles, is the magnetostatic interaction. On the other hand, the energy and character of the magnetostatic interaction are determined by the magnetization state of the particles.

In this work we experimentally investigate the magnetization curves of regular rectangular lattices of permalloy nanoparticles for different external field orientations. We demonstrate that the magnetization distribution within a single particle depends on the magnetization process and the external field orientation to the lattice axis. This is a result of the interplay of the interparticle interaction and the single-particle state. The particles can be both at single-domain and vortex states at zero field. The appearance of the magnetization vortices leads to the appearance of a remanent perpendicular magnetization, while magnetizing perpendicular to the easy axis of the system. The competition between the single-domain and vortex states in a system of two magnetostatically interacted magnetic nanodisks is numerically studied.

II. EXPERIMENT

Arrays of magnetic particles were fabricated by electron-beam lithography. The main feature of our method is the use

of a fullerene as a resistor for electron lithography. Small sizes of C_{60} molecules and the ability of the fullerene to modify its physical and chemical properties under exposure to electrons allow and to use this material for a high-resolution nanofabrication. The capabilities of C_{60} as a negative e resist was recently demonstrated by fabrication of 20–30-nm Si pillars.⁶ The main steps in the procedure of manufacturing permalloy nanoparticles are thin films deposition, exposing by an e beam, development, and two-stage etching. We used a double-layer mask containing a C_{60} film as the sensitive layer and a Ti film as the transmitting layer. Permalloy and Ti films were prepared by pulse laser evaporation on the substrate at room temperature. Fullerene films were deposited by sublimating a C_{60} powder at a temperature of 350 °C in a vertical reactor with hot walls, and cooling the holder for the substrate. Transmission electron microscopy, selected area diffraction, and x-ray diffraction of the metal and fullerene films were carried out to check the crystalline structure and the thickness of layers. Maximum sizes of the metal crystallites did not exceed 5 nm. The C_{60} films have an amorphous structure. The thickness of the magnetic layers was varied from 25 to 45 nm. The thickness of the masking films was 20 nm for the C_{60} layer and 30 nm for the Ti film.

The fullerene was patterned in a JEM-2000EX electron microscope with a scanning electron microscopy (SEM) mode by 200-kV e beam. We had the option to change the e -beam diameter from 10 nm and over. Utilizing a high-energy electron beam decreases the amount of backscattering electrons, and the shape of patterns becomes better defined. The doses of electron-beam irradiation were 0.05–0.1 C/cm², because this assures the reproducibility and uniformity of pattern sizes. Electron-beam irradiation of C_{60} films reduces the solvability of a fullerene in organic solvents. The most likely reason for the changes of the solvability is electron-induced polymerization of C_{60} molecules accompanied by partially graphitization.^{6,7} The exposed samples were developed in toluene for 1 min, and then patterns were transferred to the Ti layer by plasma etching with a CF_2Cl_2 atmosphere. The last step of the fabrication of the

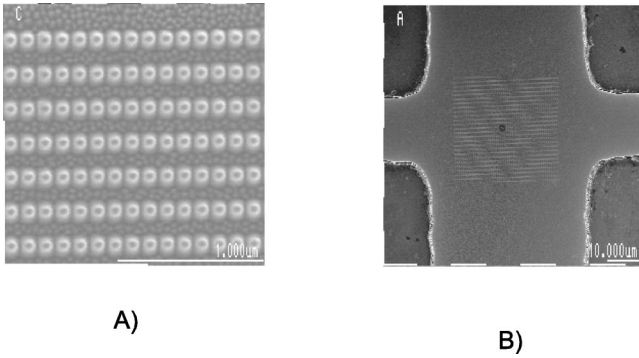


FIG. 1. The SEM image of sample 1 (see Table I). (A) The lattice of the 40–50-nm particles is visible, with a background of the 10-nm roughness of the sublayer. (B) The sample position in the Hall cross.

magnetic particles was the Ar^+ ion milling of permalloy films using this double-layered mask. Basically, the resistance of the C_{60} films to the ion milling is sufficient to use this single mask with slightly greater thicknesses, but double-etch steps are necessary to ensure a uniformity and reproducibility of the sizes of the particles. By carefully monitoring the elemental composition of the samples by means of energy dispersion spectroscopy, qualitative microanalysis, and a checking of the morphology of particles by SEM, we can better detect the final points of the plasma etching and ion milling processes. However, usually we did some overmilling at the last step, to prevent the presence of any magnetic substance between the prepared particles. One of the SEM images of the arrays of the ferromagnetic particles is presented in Fig. 1. The shape of the ferromagnetic particles is a disk, whose height is equal to the thickness of the initial permalloy film.

The parameters of the investigated samples are summarized in Table I. The symbols a and b denote rectangular lattice parameters (the distances between the centers of the particles), h is the height of the particles, and d is their diameter. The total number of the particles is equal to 10^5 .

To carry out measurements of the magnetic properties, we choose a differential Hall microsensor technique. Recently it was shown that a Hall magnetometer is a very powerful tool for investigating magnetic properties of two-dimensional (2D) nanoparticles lattices.⁸ In our work we applied a commercial magnetometer based on the Hall response in a semiconductor (InSb) to investigate the collective behavior of the fabricated 2D permalloy nanoparticle arrays. The widths of the current and voltage probes are 100 and 50 μm , respectively, and the thickness of the semiconductor layer is

TABLE I. The investigated lattices of permalloy nanoparticles: a and b are the lattice parameters, h is the height of the particles, and d is their diameter.

N	a (nm)	b (nm)	h (nm)	d (nm)
1	90	180	45	50
2	120	240	25	80

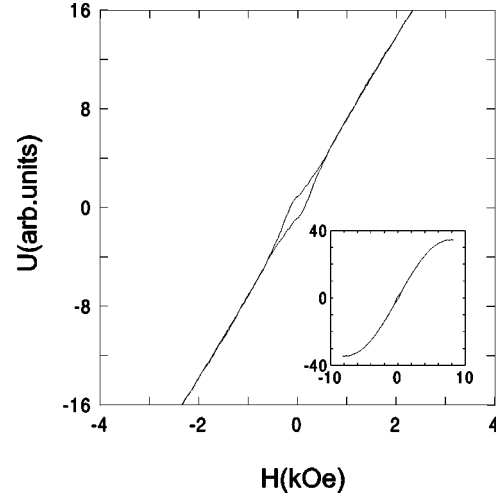


FIG. 2. The dependence of Hall signal on a magnetic field with $\theta=0^\circ$. The whole magnetization curve is shown on the casing in.

10 μm . The differential magnetometer consisted of two Hall crosses with series connections of the voltage probes. The lattice of the particles was produced in the active area of one of the Hall crosses. The difference in the Hall voltage between this sample cross and the closely spaced empty cross is measured using a bridge circuit.⁸ If the bridge is properly balanced, the resulting output voltage is proportional to the sample contribution to the perpendicular component of the magnetic field induction. The large Hall response, in combination with the good coupling of the small samples to the device, results in the excellent spin sensitivity (the signal-to-noise ratio is approximately 100). The sensor works over a large range of the magnetic field and temperature. We have investigated the magnetic properties of the samples by measuring the perpendicular magnetization as a function of the direction and magnitude of the applied field. We have carried out the investigation for three orientations of the external magnetic field: (1) the field is perpendicular to the sample plane (the polar angle is $\theta=0^\circ$); (2) the field is directed at 45° to the sample plane along the short side of the rectangle cell ($\theta=45^\circ$, the azimuthal angle $\phi=0^\circ$); and (3) the field is directed at 45° to the sample plane along the long side of the rectangle cell ($\theta=45^\circ$, $\phi=90^\circ$). The direction $\phi=0^\circ$ corresponds to the direction along the chains formed by the particles. The chains are elongated along the short side of the elementary rectangle [Fig. 1(A)]. The experimental results for the first sample for $T=4.2$ K are represented on the Figs. 2, 3, and 4.

The difference of the magnetization curves indicates the collective behavior of the system. It is a result of the magnetostatic interaction between the particles. The hysteresis if the field is directed at $\theta=45^\circ$, $\phi=0^\circ$ (Fig. 3), is an attribute of the easy axis of the magnetization which is directed along the short side of the rectangle cell. The perpendicular remanent magnetization is absent in this case. The existence of such an anisotropy in the dipole system was discussed.^{9,10} The magnetization curves if the field is directed at $\theta=0^\circ$ or $\theta=45^\circ$, $\phi=90^\circ$ (Figs. 2 and 4) are qualitatively similar. They have hysteresis in the weak magnetic field with the

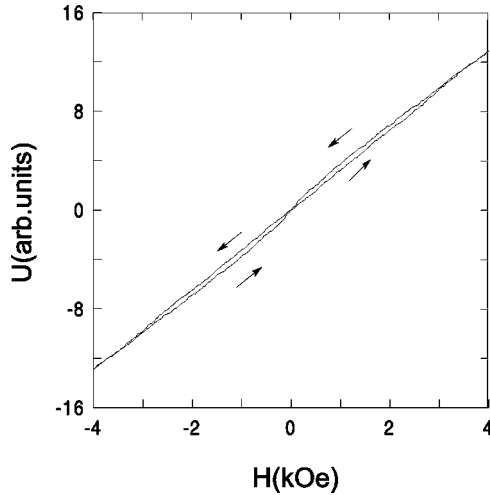


FIG. 3. The dependence of the Hall signal on a magnetic field with $\theta=45^\circ$ and $\phi=0^\circ$.

remanent magnetization. The remanent magnetization is approximately 5% of the saturation magnetization. The magnetization curves for the second sample are qualitatively similar to those of the first sample, although the samples have different shapes of the particles (see Table I). The particles have a polycrystal structure (this was determined by x-ray diffraction), and do not have the anisotropy of the form in the plane of the system. In this case the difference of the magnetization curves, for different orientation, of the external magnetic field with respect to the sample, points to the collective behavior of the particles. The existence of the anisotropy axis in the plane of the rectangular lattice was discussed earlier,^{9,10} and was expected. As for the hysteresis and the remanent magnetization of the sample with the rectangular lattice if the external magnetic field direction is $\theta=0^\circ$, $\theta=45^\circ$, or $\phi=90^\circ$, their existence seems to be unexpected. The effect cannot be explained by the properties of single particle. For noninteracting particles the remanent magnetization does not depend on the direction of the external magnetic field.

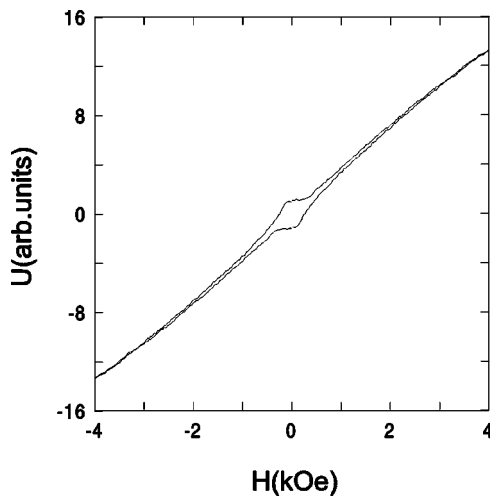


FIG. 4. The dependence of the Hall signal on a magnetic field with $\theta=45^\circ$ and $\phi=90^\circ$.

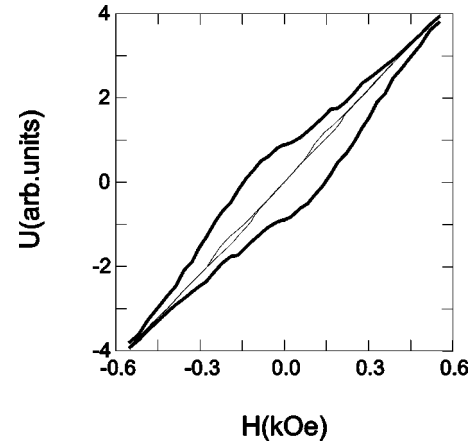


FIG. 5. The changing of the magnetization curve hysteresis with the temperature: the thick line is for 4.2 K, and the thin line for 77 K. H is directed at $\theta=0^\circ$.

The first sample was also investigated at $T=77$ K. The hysteresis if the field was directed at $\theta=45^\circ$, $\phi=0^\circ$ was not observed. The hysteresis if the field was directed at $\theta=0^\circ$ or $\theta=45^\circ$, $\phi=90^\circ$ was qualitatively changed (Fig. 5).

We suppose that the observed behavior of the system is connected with the fact that particles of the examined sizes can be in two states. The first is a single-domain state, and the second a vortex distribution of the magnetization. In the last case the core of the vortex is magnetized perpendicularly.² The interplay of the lattice anisotropy and the anisotropy of the dipole interaction between particles leads to the following behavior of the system. The particles and in the single-domain state if the external field has a component directed along the particle chains. In this case the interaction within chain has a ferromagnetic character, and therefore stabilizes the single domain state. On the other hand, if the system is demagnetized within the field perpendicular to the chains, the dipole interaction has an antiferromagnetic character within the chain, and the particles turn to be in the vortex state. As the core magnetization has its own coercivity, all cores are ferromagnetically ordered and the system has a remanent perpendicular magnetization. We performed numerical simulations to prove these suggestions.

III. NUMERICAL SIMULATION

Let us consider two magnetostatically interacting nanoparticles. This model allows one to investigate the magnetization distribution within a particle in an anisotropic system with interaction. We numerically solved a system of stochastic Landau-Lifshitz equations. The effective magnetic field takes into consideration the following components: the applied external magnetic field, the demagnetization field of the system, the field of the anisotropy and the exchange field within a particle, and the random field defined by the thermal fluctuations. An explicit Euler method was used to solve such stochastic differential equation. Note that such an approach to solve a stochastic LLH equation is well known and widely used in magnetic simulations.^{11,12} In addition, we have used the approximation of a uniform

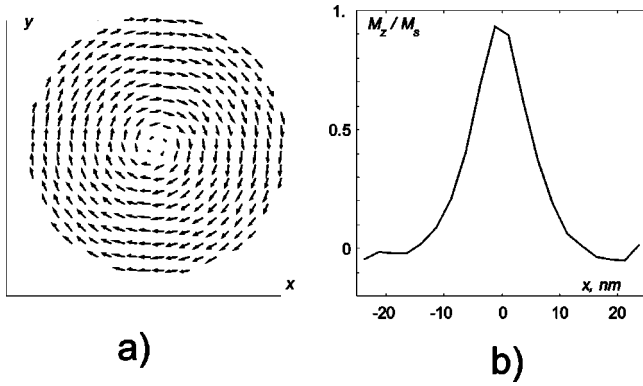


FIG. 6. (a) The vortex distribution of the magnetization in cylindrical particle. (b) The perpendicular value component of the magnetic moment.

distribution of the magnetization in the perpendicular direction. Our numerical scheme was represented in detail Ref. 13.

Let us now discuss some results of numerical experiments. First of all, for a single magnetic disk we found that the vortex magnetization state becomes a ground state only when the height and radius of the disk exceed some critical values. This fact was pointed out earlier in Ref. 14 for the square-shape particles. Figure 6 demonstrates an example of a vortex state in a cylindrical particle of diameter 50 nm and height 12.5 nm at zero external magnetic field. Note that such a state has a nonzero perpendicular component of the magnetic moment. This can lead to the appearance of a hysteresis loop in the magnetization curve in systems of magnetic particles. If there are two interacting particles, the magnetization curve is changed. Two different cases were considered: first, when the projection of the external magnetic field on the disk plane lies along the pair of particles (it corresponds to $\theta = 45^\circ$ and $\phi = 0^\circ$ in experiment), and second, when this projection lies perpendicularly to the pair (it corresponds to $\theta = 45^\circ$ and $\phi = 90^\circ$ in experiment). The diameter of the particle was 50 nm, its height was 18 nm, and the distance between the particle centers was 50 nm. The corresponding curves for the perpendicular magnetization

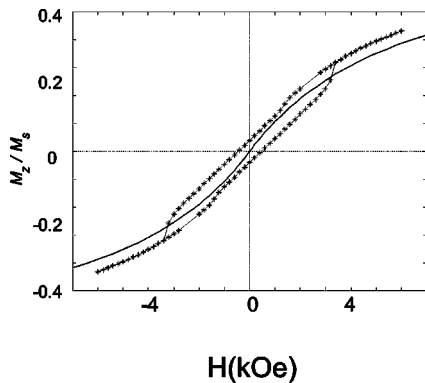


FIG. 7. Perpendicular component of the magnetization in two-particle systems at $T = 4$ K, when an external field is applied along the pair of the particles (solid line) and perpendicular to this direction (stars). The angle between the external field and the disk is 45° .

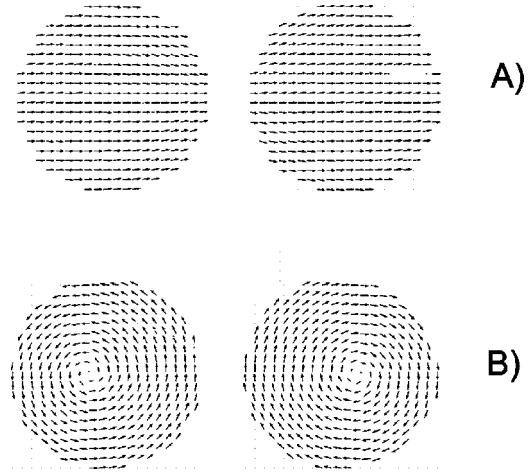


FIG. 8. The uniform (A) and vortex (B) magnetization distribution in a pair of permalloy disks.

are shown in Fig. 7. The hysteresis loop (stars in Fig. 7) is the result of a vortex penetrating into the particles at some value of the applied field. In contrast with this situation, the magnetization state remains a single domain at all values of the external field when its projection lies along the pair of the particles; as a result, the curve for a perpendicular magnetization has no hysteresis loop (Fig. 8).

IV. DISCUSSION

The following mechanism for the appearance of the remanent magnetization, implied from the results of experimental and numerical simulation, suggests an external field orientation perpendicular to the particle chain. If the external magnetic field has a component parallel to the chains, the magnetostatic interaction between particles decreases the total energy of the system, and the remanent ($H = 0$) state is uniform and the perpendicular component of magnetic moment is absent. In the case when the external magnetic field is perpendicular to the chains, magnetostatic interaction increases the total energy of the system. In order to decrease the energy of the magnetostatic interaction, the distribution of the magnetization of the particle takes a vortex form. As discussed earlier, a particle in a vortex state has a nonzero magnitude of the remanent perpendicular magnetization.

In addition, there were fundamental changes in the magnetization curve of the sample observed when the sample temperature was raised to 77 K (Fig. 5). This points to the fact that thermal fluctuations play a significant role in the system behavior, in spite of the fact that T_c of the bulk permalloy is 885 K. It is possible that the absence of the remanent magnetization at 77 K is caused by a thermally induced switching between vortex states with different polarizations.¹⁵ If the coercivity of the vortex core become less than the antiferromagnetic magnetostatic interaction between cores, the remanent magnetization of the system will be equal to zero. This hypothesis requires further theoretical investigation.

So it is shown that the interaction in a regular 2D rectangular lattice of nanoparticles plays a significant role. The interplay of the anisotropy of the magnetostatic interaction and the lattice anisotropy determines the magnetization state of the particles. It can be both a vortex state and a single-domain state. Due to the possibility of the existence of a vortex state, the system can have a rema-

nant magnetization directed perpendicularly to the system plane.

ACKNOWLEDGMENTS

We are grateful to Professor A. S. Arrott for helpful discussions. This work was supported by the RFBR (00-02-16485) and PSSNS Program grants.

*Email addresses: msap@ipm.sci-nnov.ru; sapozhnikov@anl.gov

¹R. P. Cowburn, D. K. Koltsov, A. O. Adeyeye, M. E. Welland, and D. M. Tricker, *Phys. Rev. Lett.* **83**, 1042 (1999).

²T. Shinjo, T. Okuno, R. Hassdorf, K. Shigeto, and T. Ono, *Science* **289**, 930 (2000).

³M. Schneider, H. Hoffmann, and J. Zweck, *Appl. Phys. Lett.* **77**, 2909 (2000).

⁴K. Bussmann, G. A. Prinz, S. F. Cheng, and D. Wang, *Appl. Phys. Lett.* **75**, 2476 (1999).

⁵R. P. Cowburn, A. O. Adeyeye, and M.E. Welland, *New J. Phys.* **1**, 16 (1999).

⁶T. Tada and T. Kanayama, *Jpn. J. Appl. Phys.* **35**, L63 (1996).

⁷V. M. Mikushkin and V. V. Shnitov, *Fiz. Tverd. Tela. (Leningrad)* **39**, 187 (1997) [*Sov. Phys. Solid State* **39**, 164 (1997)].

⁸A. D. Kent, S. von Molnar, S. Gider, and D. D. Awschalom, *J. Appl. Phys.* **76**, 6656 (1994).

⁹V. M. Rozenbaum, *Zh. Exp. Teor. Fiz.* **99**, 1836 (1991) [*Sov. Phys. JETP* **72**, 1028 (1991)].

¹⁰V. M. Rozenbaum, V. M. Ogenko, and A. A. Chuiko, *Usp. Fiz. Nauk* **161**, 79 (1991) [*Sov. Phys. Usp.* **161**, 883 (1991)].

¹¹A. F. Popko, L. L. Savchenko, and N. V. Vorotnikova, *Pis'ma Zh. Éksp. Teor. Fiz.* **69**, 555 (1999) [*JETP Lett.* **69**, 596 (1999)].

¹²E. D. Boerner and H. N. Bertran, *IEEE Trans. Magn.* **33**, 3152 (1997).

¹³*Fiz. Met. Metalloved. (to be published)* [*Phys. Met. Metallogr. (to be published)*].

¹⁴R. P. Cowburn and M. E. Welland, *Appl. Phys. Lett.* **72**, 2041 (1998).

¹⁵Y. Gaididei, T. Kampeter, F. G. Mertens, and A. Bishop, *Phys. Rev. B* **59**, 7010 (1999).